J. Biophotonics **3**, No. 12, 743–751 (2010) / **DOI** 10.1002/jbio.201000060

Journal of BIOPHOTONICS

FULL ARTICLE

Comparative study of tumor hypoxia by diffuse optical spectroscopy and immunohistochemistry in two tumor models

Anna V. Maslennikova[*,1,2], *Anna G. Orlova*[1], *German Yu. Golubiatnikov*[1], *Vladislav A. Kamensky*[1], *Natalia M. Shakhova*[1,2], *Aleksey A. Babaev*[3], *Ludmila B. Snopova*[2], *Irina P. Ivanova*[2], *Vladimir I. Plekhanov*[1], *Tatyana I. Prianikova*[3], *and Ilya V. Turchin*[1]

[1] Institute of Applied Physics RAS, 46 Ulyanov Str., Nizhny Novgorod, Russia
[2] Nizhny Novgorod State Medical Academy, 10/1 Minin Sqr., Nizhny Novgorod, Russia
[3] Nizhny Novgorod State University, 23 Gagarin Ave., Nizhny Novgorod, Russia

Received 25 April 2010, revised 2 July 2010, accepted 30 July 2010
Published online 18 August 2010

Key words: tumor oxygen status, hypoxia, diffuse optical spectroscopy, noninvasive diagnostics, experimental tumors

The capabilities of diffuse optical spectroscopy for noninvasive assessing of oxygen status in experimental tumors have been demonstrated. Specific features of the distribution of total hemoglobin, oxygenated hemoglobin, deoxygenated hemoglobin, and blood-oxygen saturation were shown on two tumor models having different histological structure and functional characteristics. The results obtained by the optical technique were verified by immunohistochemical study of tissue samples marked with exogenous marker of hypoxia – pimonidazole.

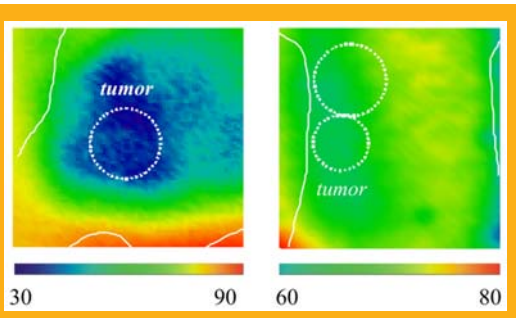

Blood oxygen saturation (%) in two tumor models: Pliss's lymph sarcoma (**a**) and rat mammary cancer (**b**).

1. Introduction

Tissue hypoxia is a powerful and independent adverse prognostic factor in solid malignancies resulting in tumor progression and resistance to therapy [1, 2]. Its influence on the disease outcome was confirmed in cervical cancer, head and neck cancer, breast cancer, and soft tissue sarcoma [3–6]. Growing comprehension of its importance for disease prognosis stimulated the development of techniques for detecting and assessing tumor oxygen status. Nowadays, the direct polarographic pO_2 probe measurement is considered to be a "gold standard" for determination of tissue oxygen status [7]. Its clinical application is restricted since it is invasive and allows evaluating pO_2 level in several tissue sites only. Immunohistochemical techniques, based on specific detection of exogenous and endogenous hypoxia markers, define localization of hypoxic and oxygenated tissue areas, indicating the relative pO_2 level [8]. The

* Corresponding author: e-mail: maslennikova.anna@gmail.com, Phone: +7(920)251-70-33, Fax: +7(831)439-09-43

possibility to obtain *ex vivo* images only appears to be the main disadvantage of this method. These limitations gave an impetus to the development of noninvasive hypoxia imaging methods. The current noninvasive approaches for *in vivo* study of tumor oxygen status include magnetic resonance imaging (MRI) and radionuclide methods (positron-emission tomography and single-photon emission computed tomography) [9, 10]. The electron paramagnetic resonance [11] as well as new imaging techniques, such as diffuse optical tomography and diffuse optical spectroscopy (DOS) [12, 13], are currently under investigation. Nevertheless, any new noninvasive imaging method should be subject to validation against the direct pO_2 probe measurement or immunohistochemical analysis to substantiate concordance with the *in vivo* microdistribution of the pO_2 level within the tumor [9].

The DOS technique is imaging modality based on reconstruction of optical characteristics of biological tissues (absorption and scattering coefficients) using information on characteristics of laser radiation transmitted through them. Spectroscopic data (obtained after irradiation of the studied object at different wavelengths) enable reconstructing component composition of tissue by absorption of the principal tissue chromophores: total hemoglobin (tHb), oxygenated hemoglobin (HbO_2), deoxygenated hemoglobin (HHb), water, and lipids. This information allows indirect evaluation of the oxygen status of biological tissues [14–16].

In this study, we tested DOS as an identifier of tissue oxygen state and verified its validity by means of immunohistochemical analysis with exogenous hypoxia marker pimonidazole. Two tumor models: rat's mammary cancer (RMC-1) and Pliss's lymph sarcoma (PLS), different in their histology and functional characteristics, were compared.

2. Materials and methods

2.1 Tumor models

The experiments were carried out on white outbreed rats. Tumor strains were purchased from the N.N. Blokhin Russian Oncological Scientific Center. Pliss's lymph sarcoma is a metastizing connective-tissue tumor [17], consisted of compact small and large irregularly shaped cellular elements with nuclei varying in shape and size. The tumor is characterized by a high mitotic activity, high cellularity, and a sufficient number of blood vessels. Rapid growth and early occurrence of necrotic areas are its distinctive features. Eleven male tumor-bearing animals were used. At the time of the experiment, the rats weighed 220 ± 10 g. The tumor was transplanted subcutaneously into the inner side of the right thigh. Experiments began after the tumor had reached 20–30 mm in diameter on the 3–5th day after strain transplantation. By this time multiple necrotic foci had been formed in the lymph sarcoma tissue.

Rat mammary cancer is an epithelial tumor with a solid structure consisting of low differentiated polymorphous cells. Its stroma is represented by thin interlayers of connective tissue with a small amount of thin-layer blood vessels [18]. The tumor is characterized by slow growth, low cellularity and late necrosis forming. White nonlinear female rats weighted about 180 ± 10 g (8 animals) were studied. RMC-1 was transplanted subcutaneously into the axillary region. Animals with the tumor node 10–30 mm in size (the 30–35th day after transplantation) were chosen for *in vivo* studies.

2.2 Diffuse optical spectroscopy

Experiments on DOS were performed on the experimental setup with parallel plane geometry (Figure 1) created at the Institute of Applied Physics RAS (Nizhny Novgorod, Russia) [19]. Three laser fibers coupled in a single bundle illuminate the studied volume at three wavelengths: 684 nm corresponding to the maximum absorption of deoxygenated hemoglobin, 850 nm corresponding to maximum absorption of oxyhemoglobin, and 794 nm at which absorption coefficients of oxygenated and deoxygenated hemoglobin coincide. In this device a high-frequency ($f_m = 140$ MHz) amplitude modulation is used, allowing determination of absorption coefficients more accurately due to separate determination of scattering and absorption coefficients. The diffuse light was detected by the Hamamatsu photomultiplier tube with an automatic gain control. Data on ab-

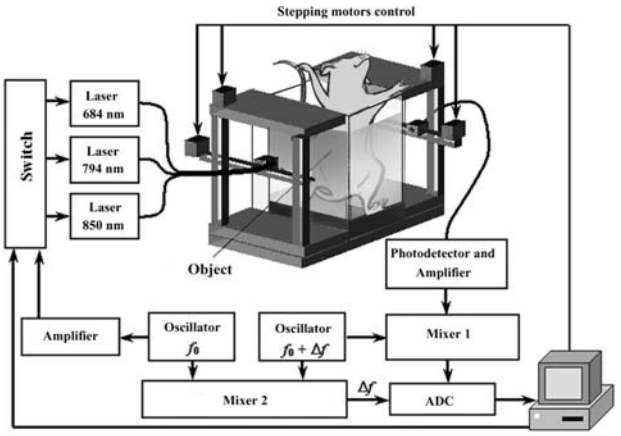

Figure 1 Schematic (block diagram) of DOS setup.

sorption at all the three wavelengths are needed for assessing the component composition of tissues. The distribution of HbO_2, HHb and oxygen saturation ($StO_2 = [HbO_2]/[HbO_2 + HHb] \times 100\%$) in tissues was reconstructed numerically.

The images were obtained by simultaneous scanning by moving the source and the detector located along the sagittal axis from the opposite sides of the studied subject with a step of 1–2 mm synchronously. Before the investigation animals were anaesthetized with intraperitoneal injection of 50 mg/kg Zoletil 100 (Virbac Sante Animale, France) and immobilized on a transparent plastic plate; the tumor region and collateral area were positioned into the scanning area. During scanning, animals were placed into a 40 mm thick cuvette containing the immersion liquid with definite optical parameters described in Section 2.3. Acquisition of one tumor image takes from 10 to 30 min depending on the tumor size and the scanning step. During the study the temperature of the immersion liquid was maintained at 37 °C. The time of signal accumulation at a point at each wavelength was about 100 ms. In each source–detector position, data were read from all the three sources.

2.3 Determination of tissue components distribution

Complex intensity of the modulated laser radiation propagating in turbid medium and registered at distance R from the source for the infinite medium can be written as follows [20]:

$$I(\beta, h) \sim I_0 \frac{\exp(-\beta R - \mathrm{i}hR)}{R} \quad (1)$$

Here, I_0 is a complex constant value (amplitude and phase) depending on the source and detector characteristics. Damping β and propagation h parameters can be written via reduced scattering μ_s' and absorption μ_a coefficients averaged over distance between source and detector:

$$\beta = \sqrt{\frac{3\mu_s'}{2}\left(\sqrt{\mu_a^2 + k_0^2} + \mu_a\right)}$$

$$h = \sqrt{\frac{3\mu_s'}{2}\left(\sqrt{\mu_a^2 + k_0^2} - \mu_a\right)}$$

where $k_0 = 2\pi f_m/c$, c is the speed of light propagation in a medium, f_m is the laser intensity modulation frequency.

For a slab geometry the boundary conditions should be taken into account and Eq. (1) can be modified according to the analytical expressions given in [21]. Solving the equation for $I(\beta, h)$ relatively β and h for each position of the source and detector one can estimate scattering and absorption coefficients averaged over depth $\mu_{a,s}(\lambda_i)$ for each wavelength, $i = 1, 2, 3$.

In fact, absorption coefficients are averaged over the sensitivity area between the source and detector (the shape of this area is shown, for example, in [22]).

The average concentrations of tissue components (HHb, HbO_2, and H_2O) C_j can be found by solving the system of linear equations

$$\mu_a(\lambda_i) = \Sigma_j(C_j \cdot \mu_j(\lambda_i))$$

where $\mu_j(\lambda_i)$ are absorption coefficients for tissue components at different wavelengths. Absolute values of $\mu_j(\lambda_i)$ are well known, they are available, for example, at http://omlc.ogi.edu/spectra/hemoglobin/. The error of tissue-component estimation in tumor depends on the fraction of tumor volume and the volume of surrounded tissue and immersion liquid in the sensitivity area. The highest error of estimation will be on the edge of the investigated object (because of the large fraction of immersion liquid in the sensitivity area) and for small tumors (because of the large fraction of 'nontumor' tissue in the sensitivity area).

It should be noted that in the described DOS system we used 3 wavelengths, which is sufficient only for a 3-component tissue model. More accurate measurements can be performed using more different light sources or using additional spectroscopic measurements [23].

To measure the I_0 value (amplitude and phase) we used a model medium with calibrated parameters that is a lipofundin solution with India ink in a transparent cuvette with different thickness (30 and 40 mm). Scattering and absorption parameters of the model medium were measured using integrating sphere and Kubelka–Munk two-flux model (the spectrophotometer Analytic Jena SPECORD 250). The error of optical parameters defining does not exceed 10%. The measurement of the I_0 factor was made before each experiment. The parameters of the immersion liquid are chosen close to the average optical properties of rat tissue [24]: 10 cm^{-1} and 0.1 cm^{-1} for the reduced scattering and absorption coefficients correspondingly for the 684 nm wavelength.

2.4 Morphological and immunohistochemical study

After scanning, tumor-bearing animals were sacrificed by administration of an overdose of intraperitoneal anesthesia, tumors were dissected and cut in

the plane of scanning. Specimens for histological study were placed in 10% neutral formalin solution. Samples were dehydrated, and then embedded in paraffin. Paraffin-embedded material was sectioned on the 5 μm thick slices using microtome Leica SM 2000 R (Germany). Slices were randomly selected from the necrosis-free areas and stained with hematoxylin and eosin. For immunohistochemical (IHC) analysis, tumor samples were shock-frozen and stored at a temperature of −135 °C; the cross sections (60 μm) were prepared using a Leica SM 200 M. Immunohistochemical analysis was done using the Hypoxyprobe^{TM}-1 kit (Hypoxyprobe, Inc., USA) following the recommendations of Natural Pharmacia International. Pimonidazole is known to be an exogenous hypoxia marker with a property of selective binding with tissues where pO_2 level is less than 10 mm Hg [25]. Monoclonal antibodies marked by fluorescein isothiocyanate (FITC) were used as a pimonidazole label. The cross sections were scanned for the FITC fluorescence signal (excitation at 488 nm, registration in the 500–540 nm range) at 100-fold magnification using LSM 510 META (Carl Zeiss GmbH, Jena, Germany). DOS results were compared with the immunohistochemical data. The standard histological study and macrospecimen analysis were also taken into consideration.

2.5 *Statistical analysis*

For the quantitative analysis of DOS results we used ratios of concentrations of tHb, HHb, HbO_2 as well as ratio of StO_2 levels in the tumor zone and contralateral region of rat body. For more accurate comparison of DOS and IHC results the quantitative estimation of relative hypoxic fraction (RHF) in two tumor models was carried out. Cross sections for this analysis were selected randomly from the central and peripheral part of the tumors. The relative hypoxic area (relationship between the square of FITC-positive areas and the common sample's square (%)) has been estimated. Data are presented as means and standard deviations. The *t*-test was performed to calculate the statistical-significance difference between correspondent parameters of two tumor models.

3. Results

Pliss's lymph sarcoma was detected as an area with amplitude of the DOS signal to be higher as compared to the contralateral extremity at all three wavelengths. Numerical reconstruction of the component composition of all studied tumors demonstrated essentially increased concentration of deoxygenated hemoglobin (Figure 2).

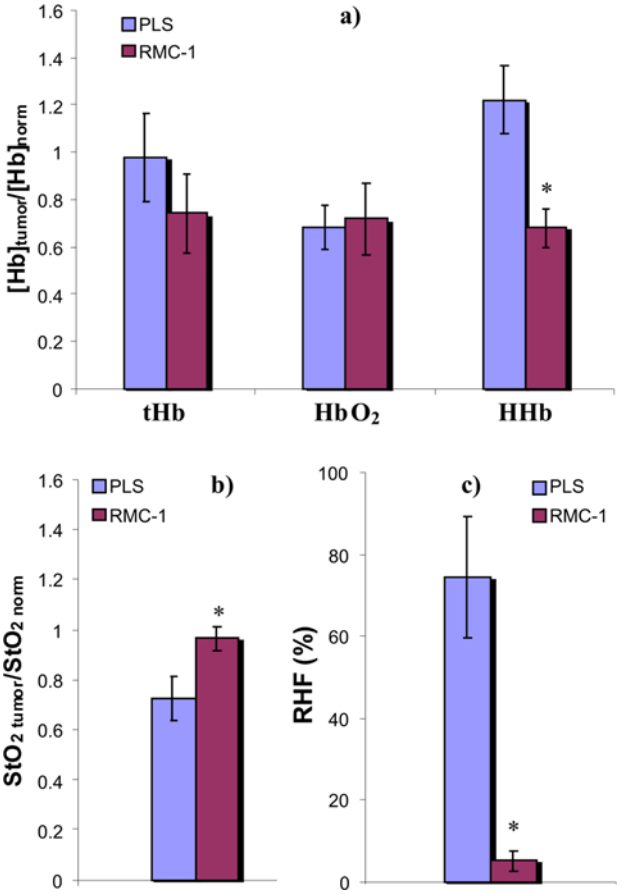

Figure 2 (online color at: www.biophotonics-journal.org) Ratios of concentrations of tHb, HHb, HbO_2 (**a**) and StO_2 (**b**) levels in tumor zone and normal area of rat body; per cent of pimonidazole positive regions (**c**) of PLS and RMC-1, $^*p$ values < 0.05.

The content of oxygenated haemoglobin of this tumor model was much lower than in the surrounding normal tissues. Total hemoglobin concentration in the tumor area was compatible with surrounding tissues. Blood oxygen saturation of PLS appears to be significantly decreased in comparison with surrounding tissues (Figure 2). A typical example of reconstructed component composition of Pliss's lymph sarcoma (tumor size 20 mm) is presented in Figure 3.

RMC-1 was also detected in DOS images as an area with signal amplitude higher than in the surrounding tissues (Figure 4a). The total hemoglobin level in this tumors was slightly reduced (Figure 2). The concentration of deoxygenated hemoglobin was close to that in the surrounding normal tissues (Figure 2). RMC-1 demonstrated the significantly decreased content of oxygenated hemoglobin (Figure 2). An example of the distribution of the principal chromo-

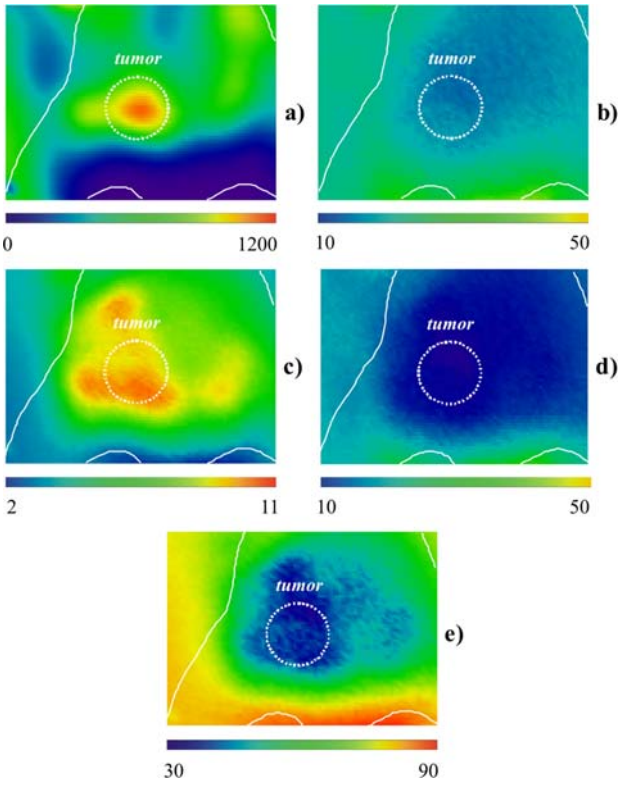

Figure 3 (online color at: www.biophotonics-journal.org) Results of DOS study of PLS area: (**a**) DOS signal amplitude (arbitrary units); distribution of the content of (**b**) total hemoglobin (μM/l); (**c**) of deoxygenated hemoglobin (μM/l); (**d**) of oxygenated hemoglobin (μM/l); and (**e**) blood oxygen saturation (%). Solid lines contour the animal body within the zone of scanning; dotted lines contour the tumor area. DOS image size 50×60 mm.

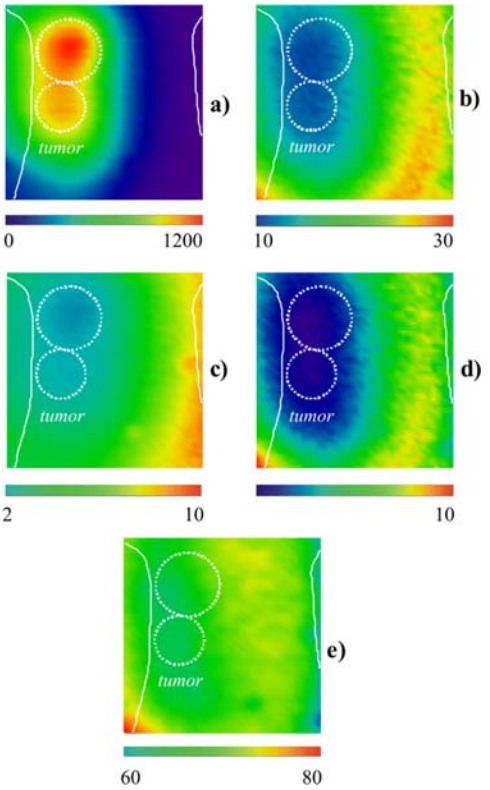

Figure 4 (online color at: www.biophotonics-journal.org) Results of DOS study of RMC-1 area: (**a**) DOS signal amplitude (arbitrary units); distribution of the content of (**b**) total hemoglobin (μM/l); (**c**) of deoxygenated hemoglobin (μM/l); (**d**) of oxygenated hemoglobin (μM/l); and (**e**) blood oxygen saturation (%). Solid lines contour the animal body within the zone of scanning; dotted lines contour the tumor area. DOS image size 50×50 mm.

phores in RMC-1 (tumor nodes sizes 20 mm and 15 mm) is given in Figure 4.

Immunohistochemical analysis confirmed the accuracy of DOS results. The characteristic feature of PLS specimens was the high level of pimonidazole uptake, which reflected the presence of extensive FITC-positive areas in all tumor samples. The sample of PLS completely stained with FITC and FITC spectra in tumor tissue are presented in Figure 5b and c. The relative hypoxic fraction of PLS was $74.6 + 14.9\%$ (Figure 2c); that confirmed the low oxygenation level.

In contrast to LSP, oxygen saturation level of RMC-1 was comparable to its values in normal tissues. Immunohistochemical study of the RMC-1 tissue samples revealed only some areas of specific FITC accumulation, alternating with FITC-negative zones (Figure 6b and c). The relative hypoxic fraction of this tumor was $5.1 + 2.4\%$ (Figure 2c); which indicated a satisfactory level of this tumor model oxygenation.

4. Discussion

Poorly oxygenated malignant tumors demonstrate a more aggressive clinical course, a higher metastatic potential, a lower survival and worse treatment response [2]. For this reason, noninvasive methods of determination of tumor tissue oxygen status play an important role for the evaluation of disease outcome, for radiation therapy planning, as well as for monitoring of the tumor response to therapy.

Assessing the oxygen status of living tissues by optical techniques is based on numerical reconstruction of tissue-component distribution. Using these techniques one can obtain indirect information about the oxygenation level of the areas of interest, but cannot determine directly the absolute pO_2 value. This study addressed the question whether the level of blood oxygen saturation obtained by DOS may be used for evaluation of oxygen status of biological tissues, in particular, different tumor models.

The research was done using two tumor models with substantially different biological properties. Fast growth, high cellularity, and early necrotization are the characteristic features of Plyss's lymph sarcoma [17]. Morphological and physiological peculiarities of this tumor suggest low level of oxygenation and the presence of broad areas of hypoxia because of its high metabolic demands. The DOS images of this tumor model demonstrated the substantially decreased level of blood oxygenation in comparison with the surrounding tissues (Figure 3e), which may be explained by increase of deoxyhemoglobin content in PLS tissue. As has been shown for normal tissues (brain and striped muscles), the rise of deoxyhemoglobin level occurs in the case of increased oxygen consumption [26, 27]. The high concentration of this substance in rapidly growing tumor with high parenchyma/stroma ratio suggests the discrepancy between the level of blood supply and the demands of rapidly growing tumor tissue. According to [28–30], this very mismatch is considered as one of the sources of chronic tumor hypoxia.

RMC-1 is a slowly growing epithelial tumor with developed stromal component, a small number of vessels and late appearance of necrotic areas [18]. DOS investigation of RMC-1 detected the oxygenation level of this tumor model, similar to the surrounding tissues (Figure 4e). There were no substantial differences between [HHb] in tumor and normal tissue that indicates relatively reduced oxygen consumption of this experimental model. Thus, in the case of slow tumor parenchyma growth, the neoplasm bloodstream can satisfy the tumor tissue need in oxygen.

A statistical comparison of [tHb], [HHb], [HbO_2] and StO_2 in PLS *vs* RMC-1 revealed that deoxyhemoglobin content was significantly higher ($p = 0.0003$) in PLS while StO_2 level was lower ($p = 0.03$); [tHb] and [HbO_2] did not demonstrate any statistical differences ($p = 0.06$ and $p = 0.67$, respectively).

The content of total hemoglobin in all studied tumors and in the surrounding tissues differed only slightly (Figure 2). There are various data concerning the amount of tHb in tumor tissues. In human neoplasms, the majority of papers report an increased content of total haemoglobin. It has been demonstrated for breast cancers [31–33] and abdomen metastases of poorly differentiated, large-cell primary lung carcinoma [34]. In tumor models, similar results were obtained for implanted kidney tumor in comparison with normal mouse kidney [35]. In the case of other well-vascularized tumor model – rat ovarian cancer – differences in tHb content between normal and neoplasm tissues were statistically significant but less then 10% (52.1 vs. 56.7 μM) [24]. In our study in the case of PLS the total hemoglobin content was comparable in normal and tumor tissues due to high levels of HHb, which is in accordance with [24]. In the case of RMC-1, which is notable for small number of blood vessels [18], total hemoglobin concen-

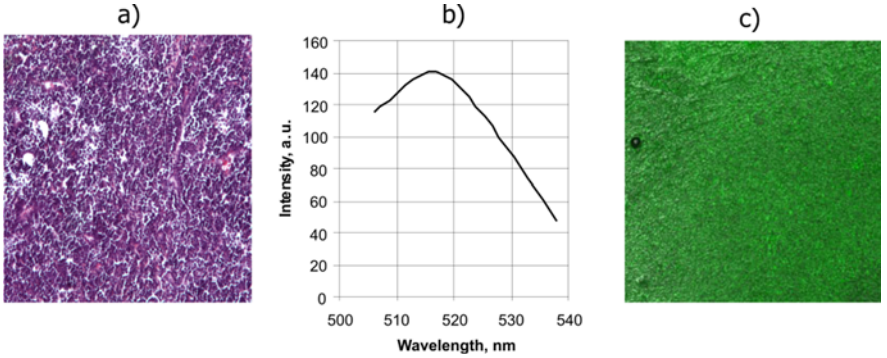

Figure 5 (online color at: www.biophotonics-journal.org) Results of PLS immunohistochemical and histological study: (**a**) histological specimen (hematoxylin and eosin ×100); (**b**) FITC fluorescence spectrum in tumor tissue; (**c**) stained immunohistochemical specimen (×100).

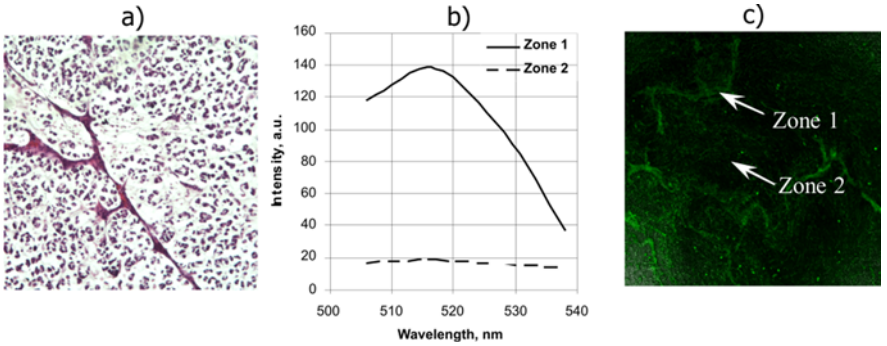

Figure 6 (online color at: www.biophotonics-journal.org) Results of RMC-1 immunohistochemical and histological study: (**a**) histological specimen stained with hematoxylin and eosin (×100); (**b**) FITC fluorescence spectrum in tumor tissue; (**c**) stained immunohistochemical specimen (×100).

tration was decreased in comparison with surrounding normal tissues. This very tumor characteristic is supposed to influence its tHb content.

Nevertheless, such a decrease of the total hemoglobin could also be a result of errors caused by the presence of a large fraction volume of the immersion liquid in the sensitivity area. In order to minimize this error we used large tumors with the tumor fraction volume in the sensitivity area more than 50%. For smaller tumors it is possible to make qualitative analysis of tumor-component changes compared with surrounding tissues. In order to perform more accurate calculations, one can use preliminary information about the tumor size and optical properties of the surrounding tissue, and making appropriate corrections for the absorption coefficients. To obtain more reliable data the more sophisticated technique – diffuse optical tomography – should be applied [36].

The validity of DOS results was tested by immunohistochemical analysis. It demonstrated a high level of pimonidazole uptake almost over the entire volume of PLS (Figure 5), whereas only some tumor areas selectively accumulating pimonidazole in RMC-1 cross sections were observed (Figure 6). A statistically significant difference between RHF ($p < 0.0001$) of two tumor models was revealed (Figure 2c). The enhanced level of RHF in PLS samples corresponds with its reduced oxygen saturation grade and indicates the hypoxic state of tumor tissue. The lowered value of RHF in RMC-1 samples corresponds with its sufficient oxygen saturation grade and indicates the normoxic state of tumor tissue. Therefore, the performed immunohistochemical investigation with exogenous hypoxia marker pimonidazole verifies the DOS results.

5. Conclusion

Our research demonstrated the capabilities of the DOS technique for *in vivo* noninvasive investigation of individual metabolic feature of tumors – its oxygenation. The immunohistochemical study with exogenous hypoxia marker verified that the DOS images adequately represent oxygen status of neoplasms. The proposed technique may be used for assessing the level of tumor model oxygenation when monitoring the tumor response to chemotherapy, radiotherapy, and photodynamic therapy.

Acknowledgements The work was done under the financial support of the Russian Foundation for Basic Research (projects No. 08-02-01042, 09-04-97063, 10-02-01142) and the Program of Basic Research of the RAS Presidium "Fundamental Sciences for Medicine". The authors are grateful to Mr. Ilya I. Fix for assistance in quantitative estimation of immunohistochemistry data and Mrs. Olga M. Leontenkova for her help in language editing.

Anna V. Maslennikova is a Professor of the department of Radiology and Radiation oncology of Nizhny Novgorod State Medical Academy, Nizhny Novgorod, Russia. She received her D.Sc. degree in 2008 in radiation oncology for the thesis "Thermoradiotherapy and chemoradiotherapy of locally advanced larynx and pharynx cancer". Her recent research interests in clinic and experiment are connected with the problem of tumor hypoxia imaging, monitoring and correction. She is the coauthor of more than 20 articles in peer-reviewed issues, 3 monographs, and 6 patents.

Anna G. Orlova is a Research Scientist of the Laboratory of Biophotonics of the Institute of Applied Physics RAS. She received her Ph.D. degree in biology in 2004 from Nizhny Novgorod State University. The major area of her research focuses on optical imaging both in clinical and experimental oncology. Her main interests include diffuse optical spectroscopy (DOS) in cancer detection as well as investigation of individual metabolic feature of tumors. In 2007 she started her scientific work directed to investigation of capabilities of DOS for tumor hypoxia imaging.

German Yu. Golubiatnikov received his Ph.D. degree in plasma physics in 1996 from Applied Physics Institute, Russian Academy of Sciences (IAP RAS), Nizhny Novgorod, Russia. Since 1983 to the present time, he was been with the Applied Physics Institute RAS, Nizhny Novgorod, and currently as a Senior Research Fellow. Recent research interests and results are in molecular spectroscopy and it application for technology; spectroscopy of biosystems.

Vladislav A. Kamensky is a Leading Scientist in the Laboratory of Biophotonics of the Institute of Applied Physics RAS. He received his Ph.D. degree in 1999 from Saratov State University. His scientific interests are connected with the area of light interactions with matter and designing novel diagnostic laser systems. He is also an Associate Professor at the Biology Department of N.I. Lobachevsky Nizhny Novgorod State University. He has more than 110 publications, monographs, conference proceedings and books of abstracts.

Natalia M. Shakhova graduated from the Nizhny Novgorod Medical Academy in 1980. She received her Ph.D. degree in 1996 and degree of Dr. of Sciences in Medicine in 2005. She is a Leading Scientist of IAP RAS and Professor of Nizhny Novgorod State Medical Academy. Her scientific interests include oncogynecology, endoscopy, laser medicine and optical bioimaging. She has more than 60 publications. In 1999 she was awarded a State Prize of the Russian Federation in Science and Technology.

Aleksey A. Babaev received his Ph.D. degree in immunology and molecular biology in 2006. He is a Senior Research Fellow of the Institute of Molecular Biology and Regional Ecology of Nizhny Novgorod State University. His research interests are focused on development of new methods of immune-enzyme analysis based on monoclonal antibodies and recombinants. He is also interested in immunohistochemical analysis of tumor tissue with endogenous and exogenous markers.

Ludmila B. Snopova is a Head of Department of Morphology of Central Research Laboratory of the Institute of Applied and Fundamental Medicine of the Nizhny Novgorod State Medical Academy, Nizhny Novgorod, Ph.D. in biology, Associate Professor. Among her research interests are the morphology and pathomorphology of tissues and organs and optical coherence tomography. She is the author of more than 120 articles and 4 patents.

Irina P. Ivanova, D.Sc. in biology, is Head of Laboratory of Physicochemical Analyses of the Institute of Applied and Fundamental Medicine of Nizhny Novgorod State Medical Academy, Nizhny Novgorod. Her main interests include cell membranes, cell biophysics, tumor physicochemical processes, photodynamic processes. She is the author of more than 10 scientific articles on this topics. In 2010 she was awarded a Honorary diploma of the Governor of Nizhny Novgorod region.

Vladimir I. Plekhanov, is a Leading Technologist of the Institute of Applied Physics, Russian Academy of Sciences, Nizhny Novgorod, Russia. The areas of his research are quantum radiophysics and laser optics. His interests are mainly concerned with design and development of optical systems for bioimaging.

Tatyana I. Prianikova, is a post-graduate student of the Department of Biomedicine, Biological Faculty, Nizhny Novgorod State University, Nizhny Novgorod. She participates in experiments on investigation of oxygen status of experimental tumors. The main area of her research is noninvasive monitoring of tumor growth under different conditions.

Ilya V. Turchin is a Head of the Biophotonics Laboratory at the Institute of Applied Physics RAS. He received his Ph.D. degree in 2006. His scientific interests are mostly connected with biomedical imaging from microscopy level to the whole-body. I. He is also an Associate Professor of Biological Faculty of the Nizhny Novgorod State University. He has more than 60 publications and 5 patents.

References

[1] J. E. Eriksen and M. R. Horsman, Radiother. Oncol. **81**, 119–121 (2006).
[2] P. Vaupel, Oncologist **13**, 21–26 (2008).
[3] M. Hockel, K. Schlenger, B. Aral, M. Mitze, U. Schaffer, and P. Vaupel, Cancer Res. **56**, 4509–4515 (1996).
[4] D. M. Brizel, S. P. Scully, J. M. Harrelson, L. J. Layfield, J. M. Bean, L. R. Prosnitz, and M. W. Dewhirst, Cancer Res. **56**, 941–943 (1996).
[5] M. Nordsmark, M. Overgaard, and J. Overgaard, Radiother. Oncol. **41**, 31–39 (1996).
[6] P. Vaupel, A. Mayer, S. Briest, and M. Hockel, Cancer Res. **63**, 7634–7637 (2003).
[7] D. K. Kelleher, O. Thews, and P. Vaupel, Radiother. Oncol. **45**, 191–197 (1997).
[8] A. Yaromina, D. Zips, H. D. Thames, W. Eicheler, M. Krause, A. Rosner, M. Haase, C. Petersen, J. A. Raleigh, V. Quennet, S. Walenta, W. Mueller-Klieser, and M. Baumann, Radiother. Oncol. **81**, 122–129 (2006).
[9] I. Serganova, J. Humm, C. Ling, and R. Blasberg, Clin. Cancer Res. **12**, 5260–5264 (2006).
[10] S. Davda and T. Bezabeh, Cancer Metast. Rev. **25**, 469–480 (2006).
[11] M. Elas, B. B. Williams, A. Parasca, C. Mailer, C. A. Pelizzari, M. A. Lewis, J. N. River, G. S. Karczmar, E. D. Barth, and H. J. Halpern, Magnet. Reson. Med. **49**, 682–691 (2003).
[12] V. Ntziachristos and B. Chance, Breast Cancer Research **3**, 41–46 (2001).
[13] C. Menon, G. M. Polin, I. Prabakaran, A. His, C. Cheung, J. P. Culver, J. F. Pingpank, C. S. Sehgal, A. G. Yodh, D. G. Buerk, and D. L. Fraker, Cancer Res. **63**, 7232–7240 (2003).
[14] A. Torricelli, L. Spinelli, A. Pifferi, P. Taroni, R. Cubeddu, and G. Danesini, Opt. Express **11**, 853–867 (2003).
[15] B. J. Tromberg, A. Cerussi, N. Shah, M. Compton, A. Durkin, D. Hsiang, J. Butler, and R. Mehta, Breast Cancer Research **7**, 279–285 (2005).
[16] B. W. Pogue, S. P. Poplack, T. O. McBride, W. A. Wells, S. K. Osterman, U. L. Osterberg, and K. D. Paulsen, Radiology **218**, 261–266 (2001).
[17] G. B. Plyss, Bull. Exp. Biol. Med. **2**, 95–99 (1961).
[18] V. P. Konoplev and N. D. Lagova, Bull. Exp. Biol. Med. **50**, 79–81 (1960).
[19] A. G. Orlova, I. V. Turchin, V. I. Plehanov, N. M. Shakhova, I. I. Fiks, M. I. Kleshnin, N. Yu. Konuchenko, and V. A. Kamensky, Laser Phys. Letters **5**, 321–327 (2008).
[20] R. C. Haskell, L. O. Svaasand, T.-T. Tsay, T.-C. Feng, M. S. McAdams, and B. J. Tromberg, J. Opt. Soc. Am. **11**, 2727– 2741 (1994).
[21] D. Contini, F. Martelli, and G. Zaccanti, Applied Optics, **36**, 4587–4599 (1997).
[22] S. B. Colak, D. G. Papaioannou, G. W. Hooft, M. B. van der Mark, J. C. J. Paasschens, J. B. M. Melissen, and N. A. A. J. van Asten, Appl. Optics **36**, 180–213 (1997).

[23] F. Bevilacqua, A. J. Berger, A. E. Cerussi, D. Jakubowski, and B. J. Tromberg, Appl. Optics **39**, 6498–6507 (2000).
[24] T. H. Pham, R. Hornung, M. W. Berns, Y. Tadir, and B. J. Tromberg, Photochem. Photobiol. **73**, 669–677 (2001).
[25] J. A. Raleigh, S. C. Chou, G. E. Arteel, and M. R. Horsman, Radiat. Res. **151**, 580–589 (1999).
[26] R. A. De Blasi, M. Cope, C. Elwell, F. Safoue, and M. Ferrari, Eur. J. Appl. Physiol. **67**, 20–25 (1993).
[27] H. Lu, X. Golay, J. J. Pekar, and P. C. M. van Zijl, Journal of Cerebral Blood Flow & Metabolism **24**, 764–770 (2004).
[28] K. L. Bennewith and R. E. Durand, Brit. J. Cancer **85**, 1577–1584 (2001).
[29] F. Zywietz, L. Bohm, C. Sagowski, and W. Kehrl, Strahlenther Onkol **180**, 306–314 (2004).
[30] D. J. Honess, Y. Kitamoto, M. R. Rampling, and N. M. Bleehen, Brit. J. Cancer **74**, S236–S240 (1996).
[31] J. Q. Brown, L. G. Wilke, J. Geradts, S. A. Kennedy, G. M. Palmer, and N. Ramanujam, Cancer Res. **69**, 2919–2926 (2009).
[32] B. J. Tromberg, O. Coquoz, J. B. Fishkin, T. Pham, E. R. Anderson, J. Butler, M. Cahn, J. D. Gross, V. Venugopalan, and D. Pham, Philosophical Transactions Royal Society London B **352**, 661–668 (1997).
[33] B. W. Pogue, S. Jiang, H. Dehghani, C. Kogel, S. Soho, S. Srinivasan, X. Song, T. D. Tosteson, S. P. Poplack, and K. D. Paulsen, J. Biomed. Opt. **9**, 541–552 (2004).
[34] J. B. Fishkin, O. Coquoz, E. R. Anderson, M. Brenner, and B. J. Tromberg, Appl. Optics **36**, 10–20 (1997).
[35] J. Masciotti, G. Abdoulaev, J. Hur, J. Papa, J. Bae, J. Huang, D. Yamashiro, J. Kandel, and A. H. Hielscher, Proceedings of SPIE **5693**, 74–81 (2005).
[36] S. Srinivasan, B. W. Pogue, B. Brooksby, S. Jiang, H. Dehghani, C. Kogel, W. A. Wells, S. P. Poplack, and K. D. Paulsen, Technol. Cancer Res. Treat. **4**, 513–526 (2005).